Hunt,
As always I would be grateful for any comments.
Colin

EUROPEAN ORGANIZATION FOR NUCLEAR RESEARCH

Addendum 6 - NPA 69-6

ON THE CALIBRATION OF THE MASS SCALES IN EXPERIMENTS ON THE K_L^o DECAY

C.A. Ramm

ABSTRACT

The calibrations of the mass scales in the runs of a K_L^o experiment have been intercompared from the positions of the high mass edge of the $(\pi^+\pi^-)$ continuum from the $K_{\pi 3}^o$ decay. These results are used to diminish the run to run fluctuations in the calibrations and thus enhance the mass resolution in data from a number of runs. The procedure is illustrated for the observation of the $K_L^o \rightarrow \pi^+\pi^-$ decays, from which an absolute calibration of the mass scales is established. Using this calibration the structure in the $M_{\mu\pi}$ spectra, attributed to the formation of heavy leptons in the K_L^o decay, appears at the same mass values as in previous observations.

(Geneva - 6 December 1971)

One of the reference phenomena which can be used for the calibration of the mass scales in K^o_L experiments is the $M_{\pi\pi}$ edge from the decay : $K^o_{\pi 3} \rightarrow \pi^+ + \pi^- + \pi^o$. The $(\pi^+\pi^-)$ pairs with the maximum invariant mass ($M_K - M_{\pi^o} = 0.3628$ GeV) are distinguishable kinematically because they have no resultant transverse momentum (p_T) with respect to the line of flight of the K^o_L. Statistically, the experimental observation of the $M_{\pi\pi}$ edge is more significant for the relative calibration of mass scales than the observation of the line from $K^o_L \rightarrow \pi^+\pi^-$.

A previous report [1] describes the intercomparison of the mean mass scales in individual runs of a K^o_L experiment [2] in spark chambers by inspection of histograms of the $M_{\pi\pi}$ edge. This report discusses an analytical means of using such histograms for the intercomparison of the mean mass scales and for diminishing the fluctuations. The results are illustrated for the observation of the $K^o_L \rightarrow \pi^+\pi^-$ decay and for the structure in the $M_{\mu\pi}$ spectrum attributed to heavy leptons.

Principles of the analysis

An example of a histogram of the $M_{\pi\pi}$ edge from 40 runs of the K^o_L experiment is shown in Fig. 1. It gives the distribution of the invariant mass of all the charged pairs from the K^o_L decay with $p_T < 0.040$ GeV/c, assigned as pions : the background due to the $K^c_{\mu 3}$ decay has been reduced by selecting only those events associated with a γ-ray indication.

The following procedure for calibration determines the relative differences between the mass scales of all the individual runs which contribute to Fig. 1, by intercomparing their $M_{\pi\pi}$ histograms in pairs. Consider the histograms from the i^{th} and j runs : if these are normal statistical distributions from the same physical phenomenon then the calibration of their mass scales can be compared by noting their relative displacement in the superposition for which they show the best

coefficient of correlation (X^2). This coefficient has been measured by the relation :

$$X^2 = (I + J)\left[\frac{1}{I} \sum_{l=1}^{k} \frac{I_l}{I_l + J_l} + \frac{1}{J} \sum_{l=1}^{k} \frac{J_l}{I_l + J_l} - 1 \right]$$

where I_l and J_l are the contents of the l^{th} bins of the superposed range of k bins of the histograms i and j. In this range the histograms contain totals of I and J events, respectively. Asymptotically X^2 becomes χ^2 for k-1 degrees of freedom.

There are two possible ways of determining the superposition of best correlation : either the various X^2 can be calculated when the range of k consecutive bins of the histogram i is superposed in all possible positions on j and the lowest value X^2_{ij} retained, or the same calculations can be made when the range k is interchanged with respect to i and j and the lowest value X^2_{ji} is retained. The number of bins of displacement with respect to the range k of the respective mass scales for the superpositions which give X^2_{ij} and X^2_{ji} will be denoted by d_{ij} and d_{ji} ; only displacements of an integral number of bins are considered.

The results from the intercomparison of all possible pairs of histograms of the $M_{\pi\pi}$ edge can be represented according to their run number n as a square matrix :

n → / ↓	1	2	3	4	.	N
1	0	d_{12}	d_{13}	d_{14}	.	.
2	d_{21}	0	d_{23}	d_{24}	.	.
3	d_{31}	d_{32}	0	d_{34}	.	.
4	d_{41}	d_{42}	d_{43}	0	.	.
.	.	.	.	.	0	.
N	.	.	.	.	.	0

Representations of the relative calibrations of the mass scales in the N histograms, in terms of the bin width, are given by either the sums of each of the N rows or by the sums of each of the N columns of the matrix :

$$(D_1)_i = \left(\sum_{n=1}^{N} d_{ij} \right)/(N - 1)$$

$$- (D_2)_i = \left(\sum_{n=1}^{N} d_{ji} \right)/(N - 1)$$

Thus $(D_1)_i$ is a measure of the relative position of the mass scale of the i^{th} histogram obtained with the range k of each of the other histograms at the best superposition. Similarly $(D_2)_i$ is obtained when the range k of the i^{th} histogram is at the best superposition on each of the other histograms.

Example of the calibration

In the determination of the $(D_1)_i$ and the $(D_2)_i$ the range k must be defined for each histogram ; for this example the 30 bins in each histogram in the mass range : $0.340 < M_{\pi\pi} < 0.370$ GeV, indicated in Fig. 1, have been used. It has been found that the type of results obtained is not specific to the precise choice of either k or the limit on p_T.

The set of $(D_1)_i$ and $(D_2)_i$ from the 40 runs of the spark chamber experiment are shown in Fig. 2. For the purposes of illustration the data from the 1970 runs have been used before the application of the result of a magnetic field calibration which leads to a momentum correction of $\Delta p = + 0.0016\ p$ in the final data reduction. The diagram shows that the average calibration of the mass scales of the 1970 runs tends to be lower than those of 1969. After applying the momentum correction, the same analysis gives the result shown in Fig. 3 ; the average calibrations of the 1969 and 1970 mass scales are evidently closer than in Fig. 2.

In these figures it can be seen that in general $(D_1)_i \sim (D_2)_i$, i.e. approximately the same relative position of the mass scale for the i^{th} histogram is found independently of whether the range k is in that histogram or in all the others. Therefore the relative changes in position, from run to run, of the $M_{\pi\pi}$ mass scales can be studied in terms of the mean (D_i) of $(D_1)_i$ and $(D_2)_i$.

These D_i from Figs. 2 and 3 are shown in (a) and (b) of Fig. 4. Apart from the displacement associated with the magnetic field correction the relative positions of the D_i are similar in (a) and (b) ; this indicates an insensitivity of the analysis to the redistribution, produced by the correction, of the statistical fluctuations due to the changes in the bin positions in the 1970 histograms.

A comparison between the relative positions of the $M_{\pi\pi}$ edges obtained previously by inspection [1] and the results of Fig. 4a is shown in Fig. 5. The two sets of results have a certain correlation and extend over similar mass intervals ; a detailed correlation cannot be expected because of the lower precision of the preliminary calibration by direct inspection of the $M_{\pi\pi}$ edge.

Fluctuations in the mass scale calibrations

The times at which the changes in the relative calibrations of the mass scales occur during the experiment are in general unknown ; no correlation between the mass scale calibration and the run numbers is evident from the diagrams. Therefore, unless the changes in calibration are always large and more frequent than the changes in run numbers, it seems plausible to suppose that sequences of runs with similar values of D_i might have higher mass resolution than the others ; potentially in such runs the differences between the mean mass scale calibration and the instantaneous calibrations may be less than in sequences of runs with larger variations in D_i.

A test of this hypothesis with the signal due to the $K_L^o \to \pi^+\pi^-$ decay is shown in Fig. 6a, the $(\pi^+\pi^-)$ pairs have been selected with $p_T < 0.010$ GeV/c. The shaded histogram comes from the runs with their D_i joined by heavy lines in Fig. 4b, the other histogram is from the remaining runs. Both histograms show the $K_L^o \to \pi^+\pi^-$ signal ; the mass resolution from the selected runs is higher than in the remainder, a result which is compatible with the hypothesis.

Reduction of the mass scale fluctuations

The spread in the D_i from the 40 runs can be diminished by an appropriate momentum correction for each run, analogous to the magnetic field correction for the 1970 runs already illustrated in Fig. 3. Such a procedure cannot increase significantly the mass resolution in the individual runs ; however, in the cases where there are only small differences between the calibration of the mean and instantaneous mass scales, it may increase the mass resolution in data collected from a number of runs.

A correction $(\Delta p)_i = 0.007\ p\ D_i$ has been used to diminish the differences in calibration. This has little effect on the mean position of the $M_{\pi\pi}$ mass edge, as is shown in the dashed histogram in Fig. 1. The effect on the distribution of the $(D_1)_i$ and the $(D_2)_i$ can be seen in Fig. 7 : this should be compared with Fig. 3 which shows the corresponding distribution before correction. After correction most of the residual relative displacements of the $M_{\pi\pi}$ edges are < 1 MeV.

Fig. 6b shows the effect of the correction on the $K_L^o \to \pi^+\pi^-$ signal ; a comparison with Fig. 6a shows that the selected data gives a signal which is more symmetrical about the nominal K_L^o mass in (b) than in (a). This result can be advantageous for the study of structure in a spectrum. From (b) it can also be seen that near M_{K^o} the precision of absolute calibration of the mean mass scale in this selected data is about $\pm$ 0.002 GeV.

Such a precision of absolute calibration makes it interesting to compare the position of some of the structure in the $M_{\mu\pi}$ spectra in this experiment with previous observations in K_L^o experiments with absolute calibrations of the mean mass scales of comparable precision.

The structure in the $M_{\mu\pi}$ spectra

The structure in the $M_{\mu\pi}$ spectra in the range $0.422 < M_{\mu\pi} < 0.427$ GeV $(L < M_{\mu\pi} < H)$ has been first noticed from a comparison of K_L^o data with data from neutrino experiments. It is attributed to the formation of a neutral heavy lepton $(M^*_{\mu\pi})$ which is formed in the K_L^o decay : $K_L^o \rightarrow M^*_{\mu\pi} + \bar{\nu}$ and which is short lived : $M^*_{\mu\pi} \rightarrow \mu^- + \pi^+$; with corresponding processes for $\bar{M}^*_{\mu\pi}$. There are also experimental indications compatible with the existence of a charged mode of this type of particle. From a previous study [3] of data with a known calibration of the mean mass scales a weighted mean mass for the $M^*_{\mu\pi}(429)$ was determined to be 0.429 ± 0.002 GeV.

It is difficult in these experiments to identify muons and pions with certitude over a wide range of momentum. Heavy leptons of the type of $M^*_{\mu\pi}(429)$ can be detected in the $(M_{\mu\pi})_1$ spectrum, which is obtained by assigning the pairs of charged particles from the K_L^o decays so that the member of the pair with the higher transverse momentum is the muon. Various types of $M_{\mu\pi}$ spectra, obtained from samples of the 1969 data from this experiment, have been discussed [4].

Histograms of $(M_{\mu\pi})_1$ from the runs giving the shaded histogram in Fig. 6a, i.e. from the selected runs before the application of the correction $(\Delta p)_i = 0.007\ p\ D_i$, are shown in Fig. 8. Only those events are retained for which the transverse momentum of the assigned muon is greater than 0.75 of the maximum possible [4] for the calculated $M_{\mu\pi}$. A comparison of these spectra with those previously observed in the region L to H

shows a similarity. However, the structure is of low statistical significance, as can be seen from the χ^2 variation of the fits of all possible sets of five consecutive bins to the least squares fitted mean.

When the mass scale fluctuations are diminished by the correction already described, the $(M_{\mu\pi})_1$ histograms of Fig. 8 are transformed into those in Fig. 9. Of the various fluctuations about the fitted mean, those in the region L to H have the least probability of being due to statistical fluctuations, the largest value of χ^2 from the fit of five consecutive bins represents a probability of $\sim 5 \times 10^{-5}$. The largest fluctuation occurs in the bin $0.4275 < M_{\mu\pi} < 0.430$ GeV, this is compatible with the previous observations attributed to the $M^*_{\mu\pi}(429)$. The 1970 histogram is shown separately because it is a new observation with respect to those described in ref. 4.

There is no known decay of the K^o_L from which $(\pi\pi)$ pairs assigned as $(\mu\pi)$ pairs can give a significant background to the $M_{\mu\pi}$ spectrum in the region L to H. That the observed structures are not due to incorrectly assigned $(e\pi)$ pairs is demonstrated in Fig. 10, for which the events in the data of Fig. 9 which are associated with an electron or γ-ray signal have been removed.

These results are compatible with previous observations ; they also show that precision similar to that of the absolute calibration of the $M_{\pi\pi}$ mass scale near M_{K^o} also obtains in the $M_{\mu\pi}$ mass scale near 0.429 GeV. It is of interest to note that there should be a similarity between the shape and position of the K^o_L line in Fig. 6a and the region of the $M_{\mu\pi}$ spectra in Figs. 8 and 10 which, after correction of the residual fluctuations, transforms into the enhancement attributed to the $M^*_{\mu\pi}(429)$: all the mass scales in the data will contain a scaling of the actual displacements of the $M_{\pi\pi}$ edge. The data are insufficient to reach a conclusion about the shapes, the positions are displaced in the same directions.

It is outside the aim of this report to discuss further the origins of the structure in the $M_{\mu\pi}$ spectra.

Conclusion

This method of calibration of the mass scales of the runs from the spark chamber experiment [2], with reference to the $M_{\pi\pi}$ edge from the $K^o_{\pi 3}$ decay, permits the selection of a data sample in which the mass resolution of the line from $K^o_L \to \pi^+\pi^-$ is higher than in the remainder. By momentum corrections proportional to the relative displacements of the $M_{\pi\pi}$ edge the mass scale fluctuations can be diminished ; which leads to an increase in the mass resolution in the selected data that is advantageous for the study of the structure in the $M_{\mu\pi}$ spectra. In principle a still higher mass resolution could be achieved in the collective data if any correlations between the occurrence of the mass scale fluctuations and the event sequence were known.

Some of the reasons for the experimental difficulty of the study of the structure in the $M_{\mu\pi}$ spectra from the K^o_L decay are evident from this analysis. Run to run fluctuations in the calibrations of the mean mass scales which are unimportant in the usual studies of the K^o_L modes of decay, can reduce the structure in the $M_{\mu\pi}$ spectra to statistical insignificance.

Acknowledgements

It is a pleasure to acknowledge that this study has been made possible by the generous collaboration of the group [2] responsible for the K^o_L spark chamber experiment. I am especially grateful to my colleague P.G. Innocenti, from that group, who translated the data tapes and gave me the help and advice which is essential for their use.

It is also a pleasure to acknowledge and thank Mrs. H. Cabel for her continued collaboration with the data analysis.

References

(1) C.A. Ramm - A preliminary comparison of two series of spark chamber observations of the K_L^o decay. CERN NPA-69-6, Add. 5 (August 1971).

(2) C.Y. Chien, B. Cox, L. Ettlinger, L. Resvanis, R.A. Zdanis, E. Dally, P. Innocenti, E. Seppi, C.D. Buchanan, D.J. Drickey, F.D. Rudnick, P.F. Shephard, D.H. Stork, H.K. Ticho - A measurement of the form factors for the decay $K_L^o \rightarrow \pi \mu \nu$ Physics Letters 33 B, 627 (1970).

(3) C.A. Ramm - On the possible existence of heavy leptons, Nature 227, 1323 (1970).

(4) C.A. Ramm - A new test for the formation of heavy leptons in the K_L^o decay. CERN NPA 69-6, Add. 4 (May 1971).

Figure captions

Fig. 1 $M_{\pi\pi}$ edge from $K_{\pi 3}^o$ for $p_T < 0.040$ GeV/c. The histogram with the solid lines is from all the runs of the experiment, the dashed lines are referred to in the text.

Fig. 2 Distribution of the D_{ij} and D_{ji} before the application of the magnetic field correction to the data from the 1970 runs.

Fig. 3 Distribution of the D_{ij} and D_{ji} in the reduced data.

Fig. 4 a) The distribution of run number and D_i corresponding to Fig. 2.

b) The distribution of run number and D_i corresponding to Fig. 3.

Fig. 5 Comparison between the D_i of Fig. 4a and the position of the D_i determined previously by inspection.

Fig. 6 a) $M_{\pi\pi}$ spectrum near $M_{K_L^o}$ for $p_T < 0.010$ GeV. The shaded histogram is obtained from the runs joined by solid lines in Fig. 4b, the clear histogram from the other runs.

b) Result of diminishing the mass scale fluctuations on the data selection of (a).

Fig. 7 Distribution of the D_{ij} and D_{ji} after diminishing the mass scale fluctuations.

Fig. 8 a) Histogram of the $(M_{\mu\pi})_1$ spectra from the runs joined by solid lines in Fig. 4b.

b) Contribution to (a) from the 1970 experiment. The points show least squares fitted polynomial means. The χ^2 variation is for the fit of all sets of five consecutive bins of (a) to the mean.

Fig. 9 The same data as in Fig. 8, after diminishing the mass scale fluctuations.

Fig. 10 a) The same data as in (a) in Fig. 9 after removing the events associated with an electron or γ -ray signal.

b) The same data as in (a) in Fig. 8 after removing the events associated with an electron or γ -ray signal.

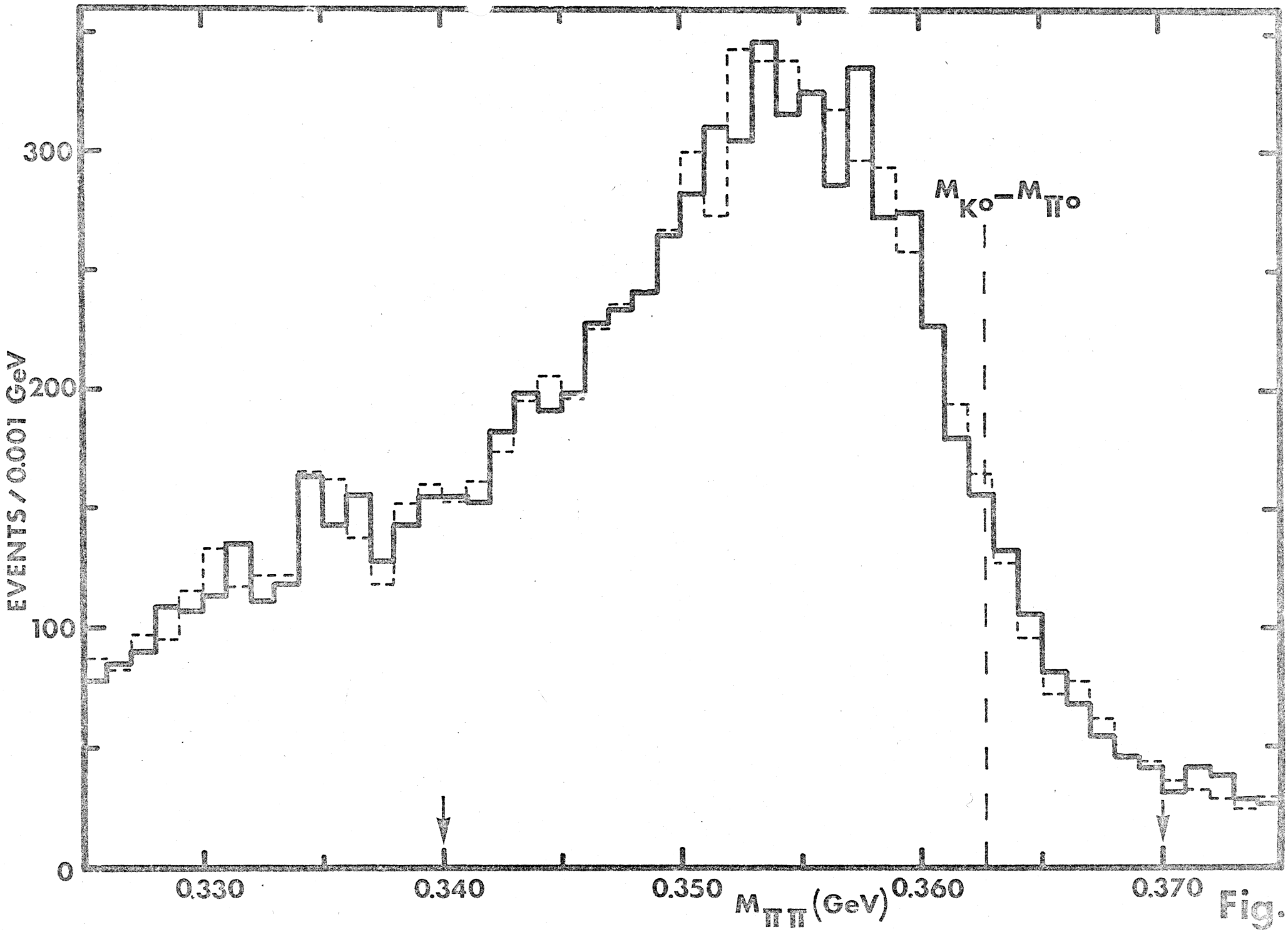
300
200
100
0
EVENTS / 0.001 GeV
$M_{K^0} - M_{\pi^0}$
0.330
0.340
0.350
0.360
0.370
$M_{\pi\pi}$ (GeV)

Fig. 1

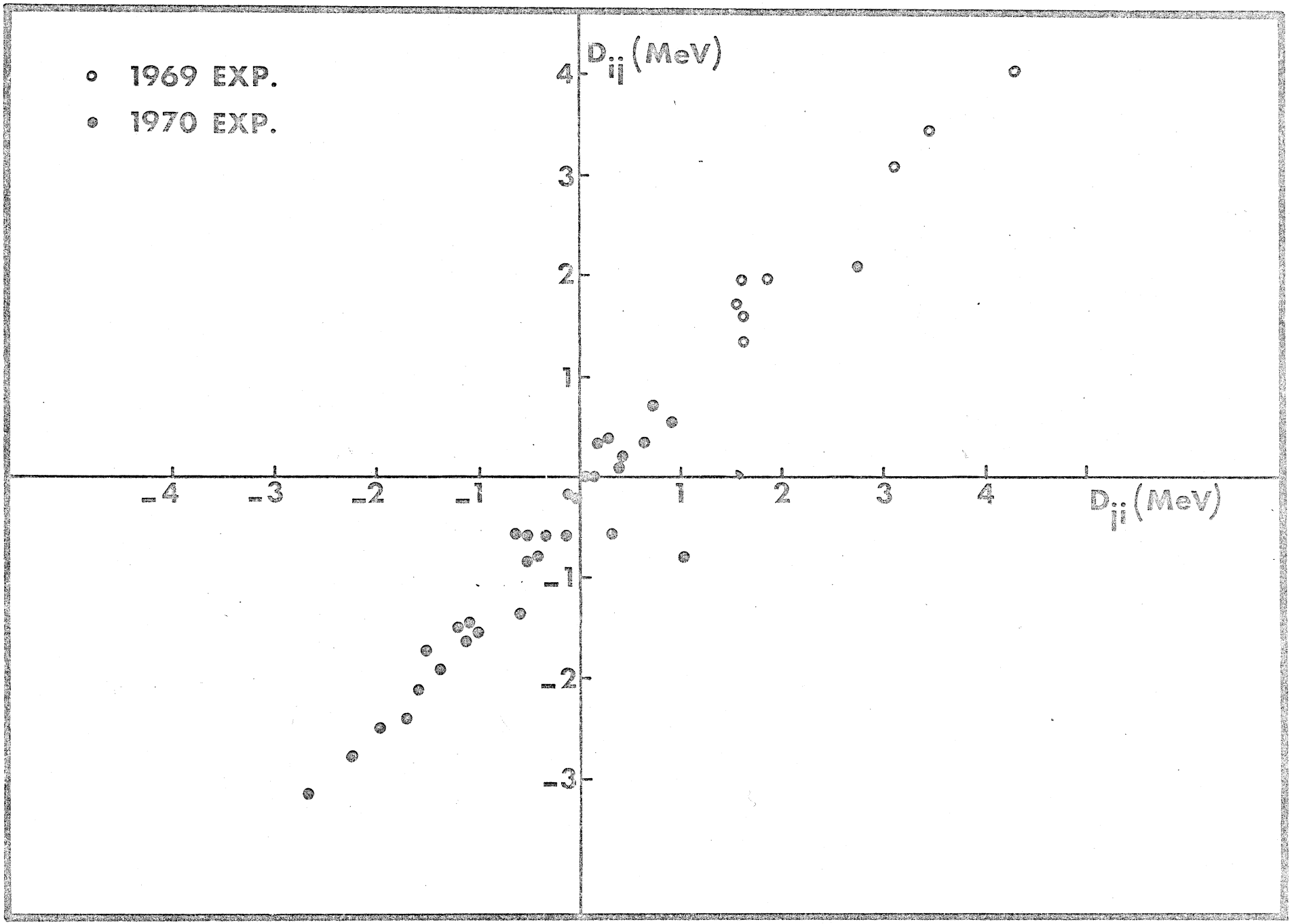

Fig. 2

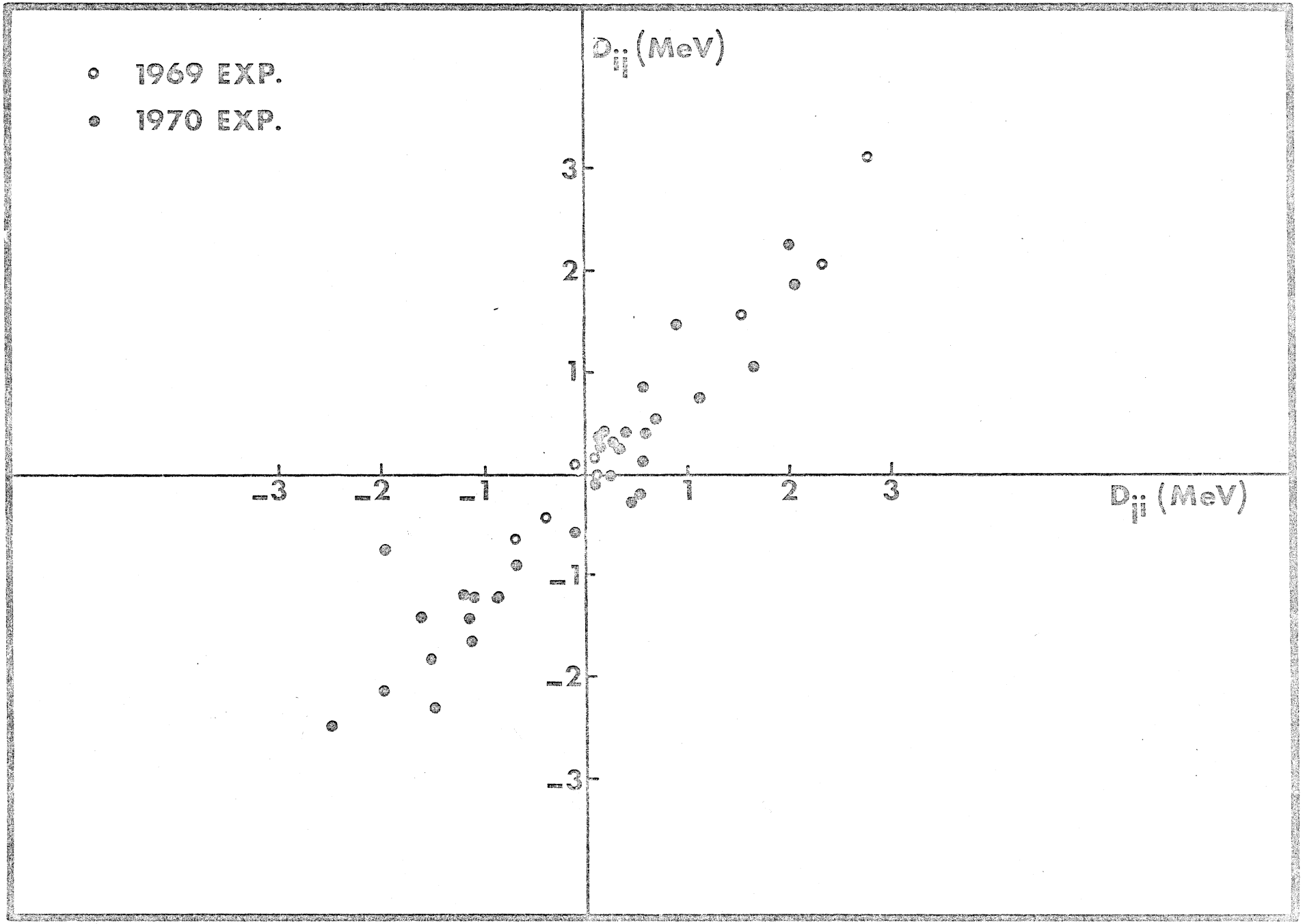

Fig. 3

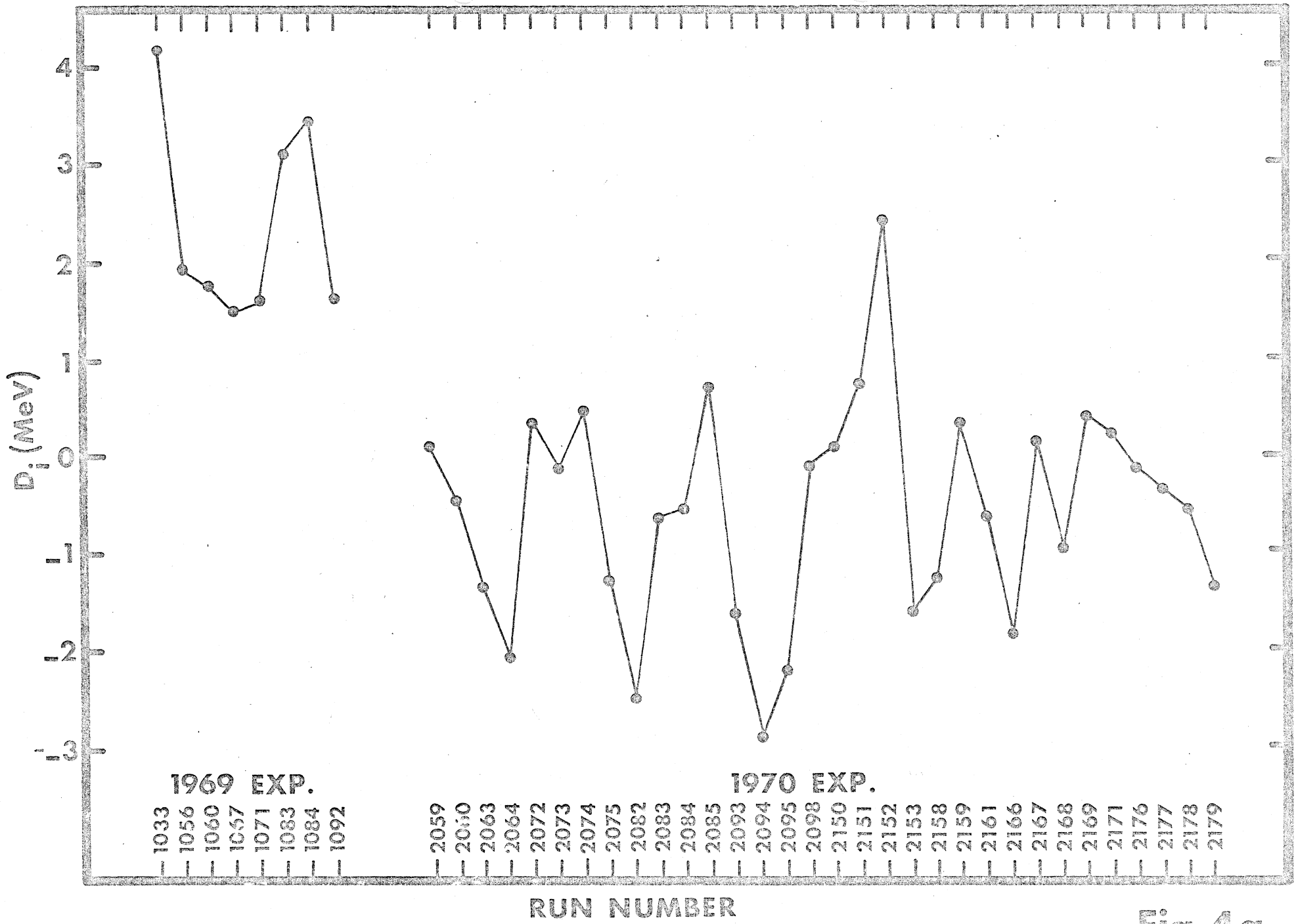
4
3
2
1
0
-1
-2
-3
D_i (MeV)
1969 EXP.
1033
1056
1060
1067
1071
1083
1084
1092
1970 EXP.
2059
2060
2063
2064
2072
2073
2074
2075
2082
2083
2084
2085
2093
2094
2095
2098
2150
2151
2152
2153
2158
2159
2161
2166
2167
2168
2169
2171
2176
2177
2178
2179
RUN NUMBER

Fig. 4a

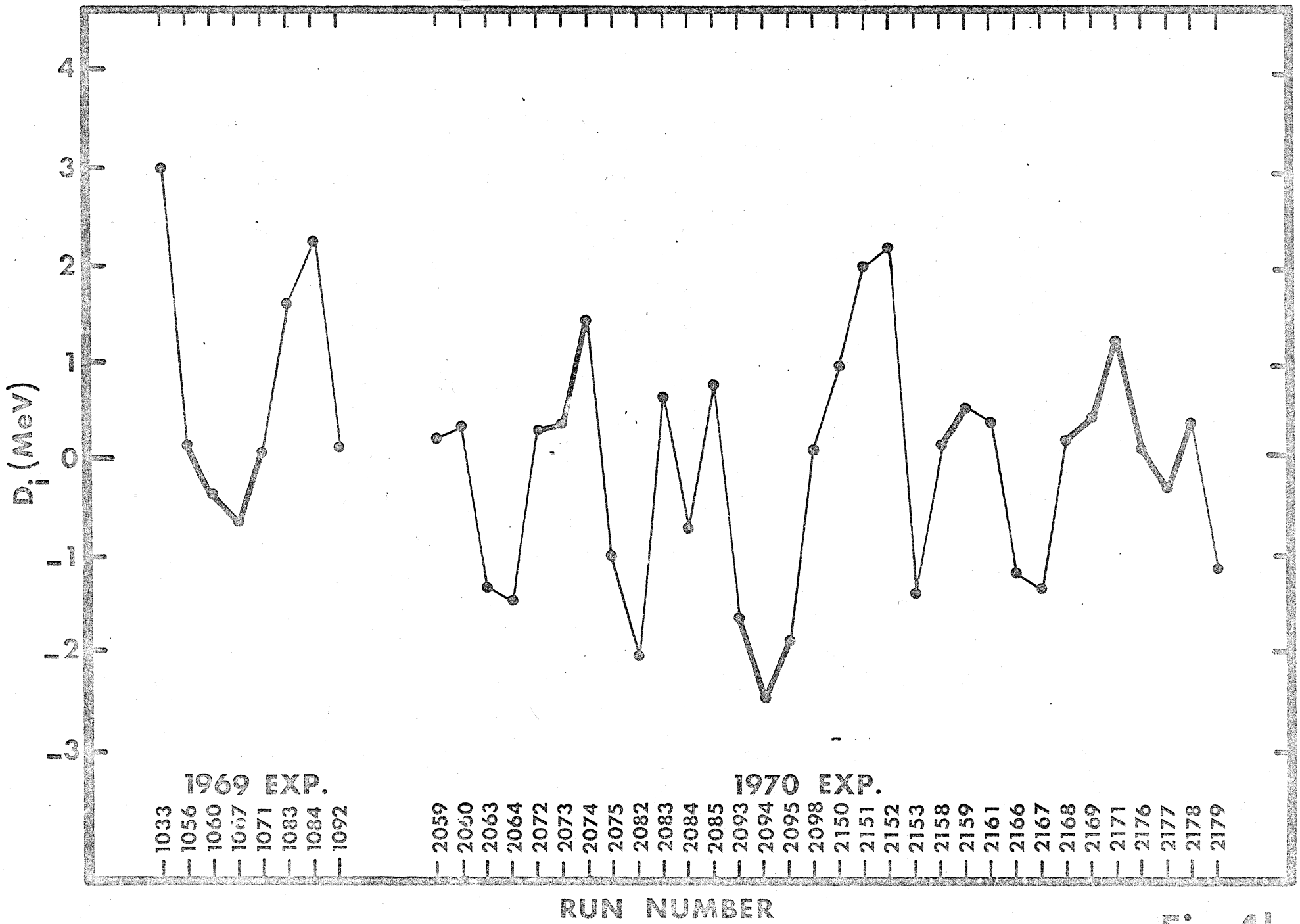
4
3
2
1
0
-1
-2
-3
D_i (MeV)
1969 EXP.
1970 EXP.
1033
1056
1060
1067
1071
1083
1084
1092
2059
2060
2063
2064
2072
2073
2074
2075
2082
2083
2084
2085
2093
2094
2095
2098
2150
2151
2152
2153
2158
2159
2161
2166
2167
2168
2169
2171
2176
2177
2178
2179
RUN NUMBER

Fig. 4b

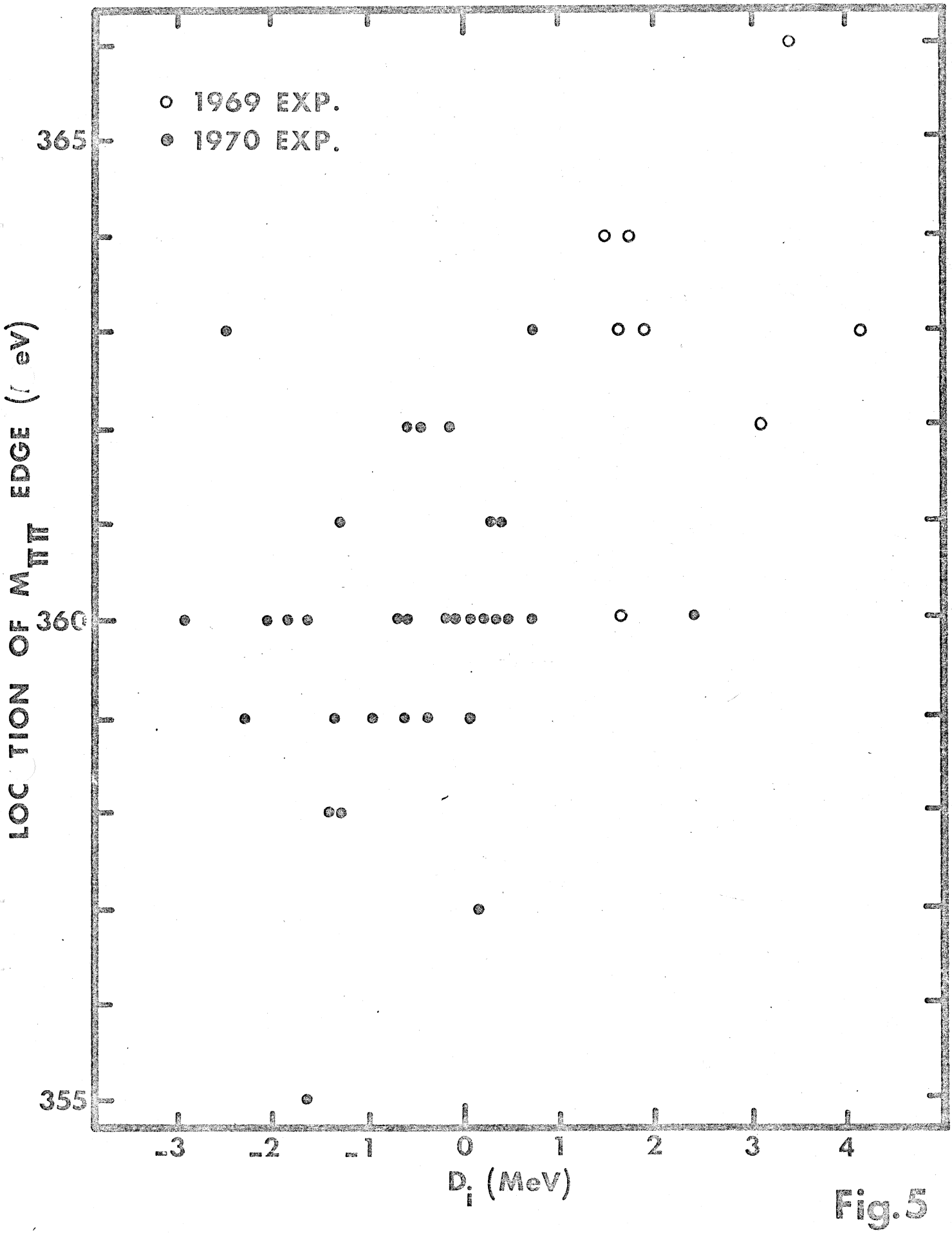
o 1969 EXP.
• 1970 EXP.
365
360
355
LOCATION OF M_{TTT} EDGE (keV)
-3
-2
-1
0
1
2
3
4
D_i (MeV)

Fig.5

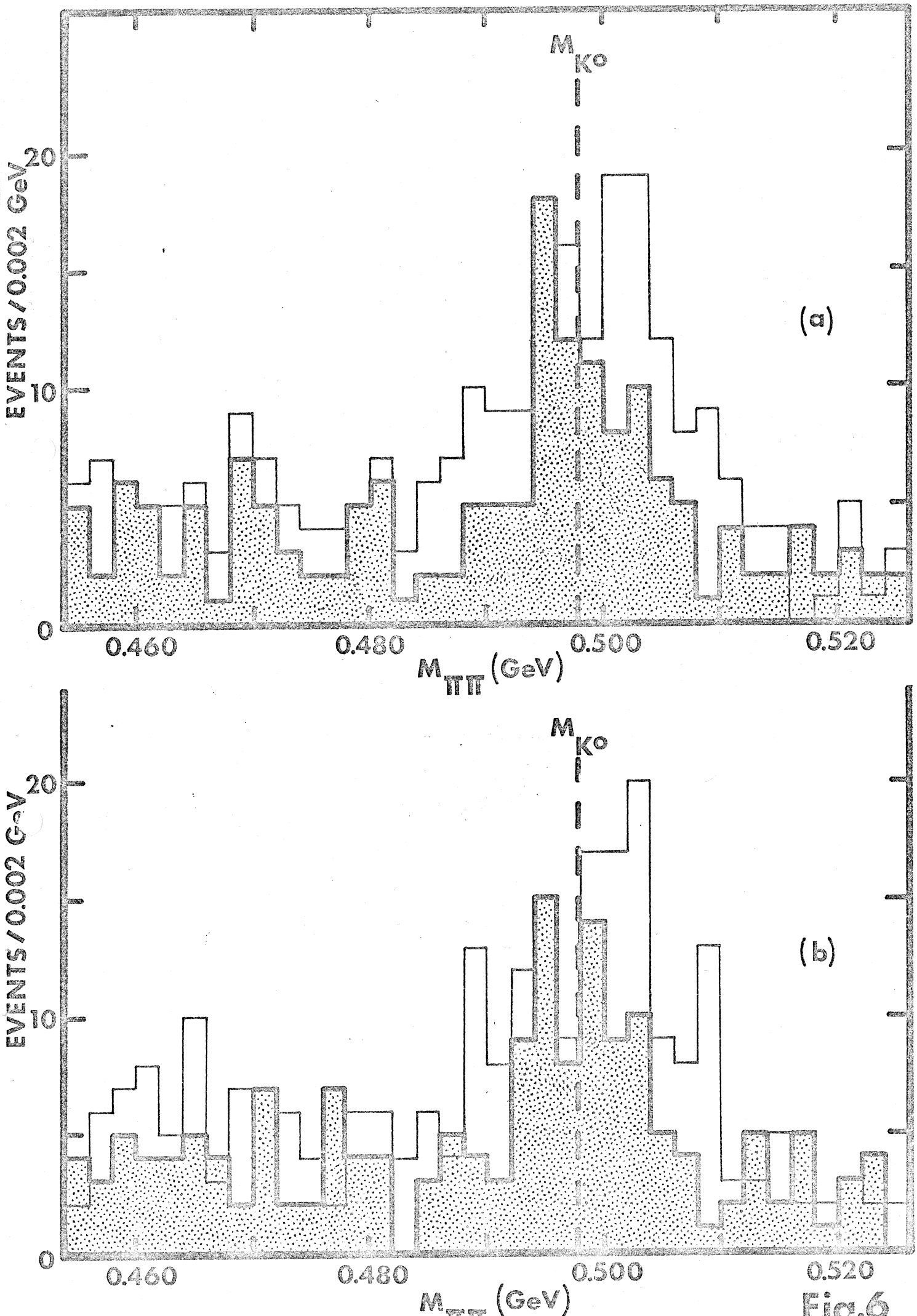
M_{K^0}
EVENTS / 0.002 GeV
20
10
0
(a)
0.460
0.480
0.500
0.520
$M_{\pi\pi}$ (GeV)
M_{K^0}
EVENTS / 0.002 GeV
20
10
0
(b)
0.460
0.480
0.500
0.520
$M_{\pi\pi}$ (GeV)

Fig.6

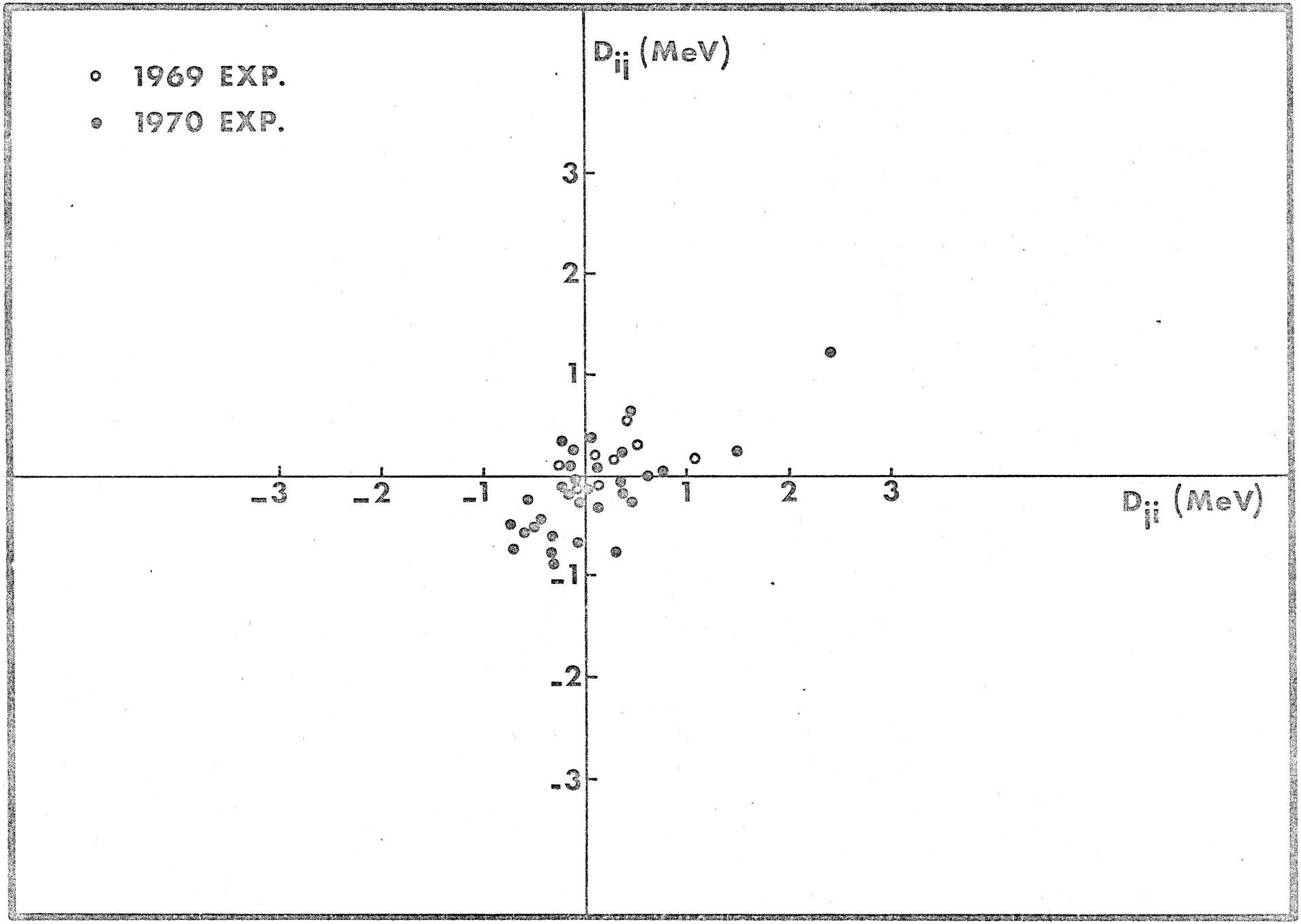

Fig.7

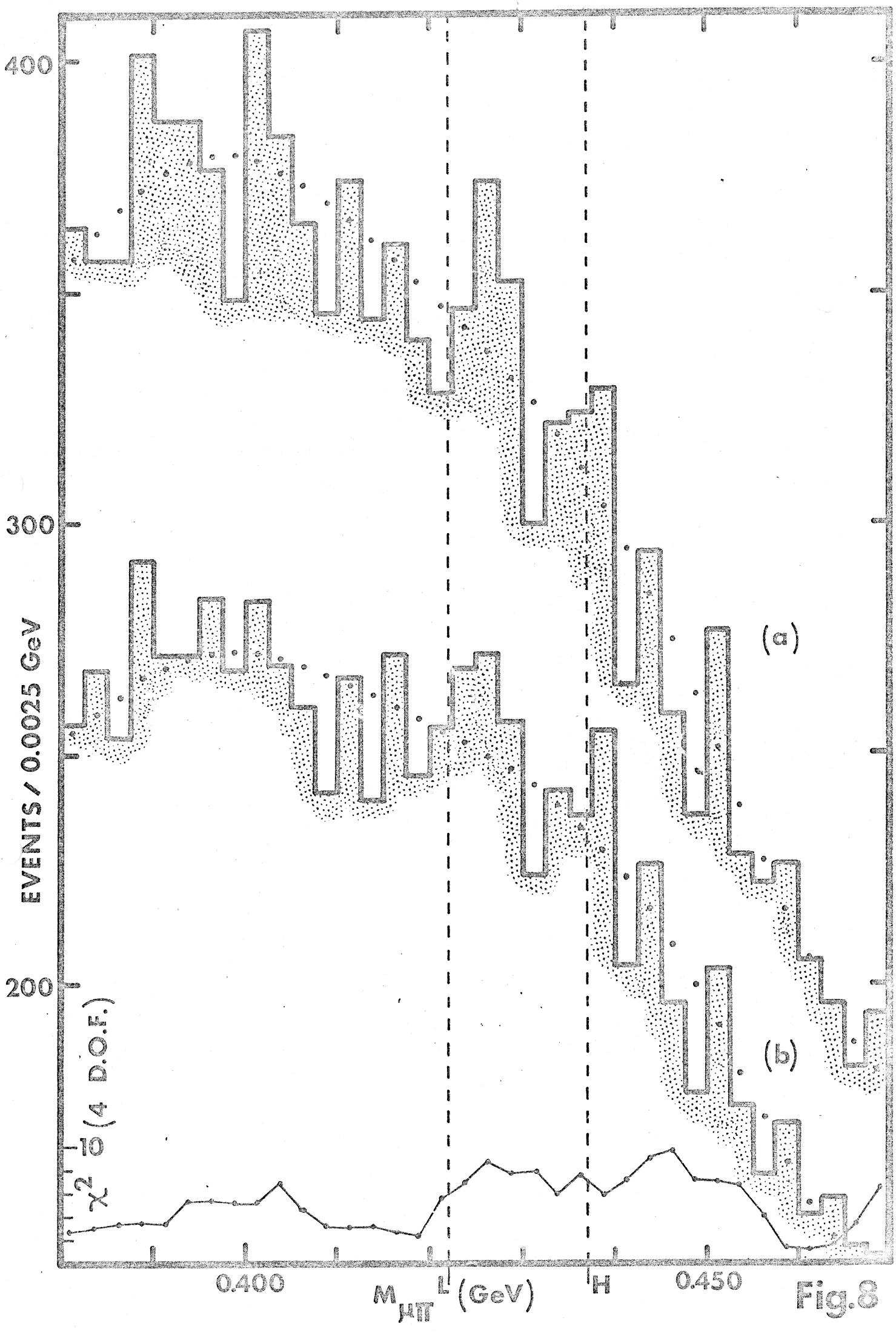
400
300
200
EVENTS / 0.0025 GeV
(a)
(b)
10
2
χ² (4 D.O.F.)
0.400
L
H
0.450
$M_{\mu\pi}$ (GeV)

Fig.8

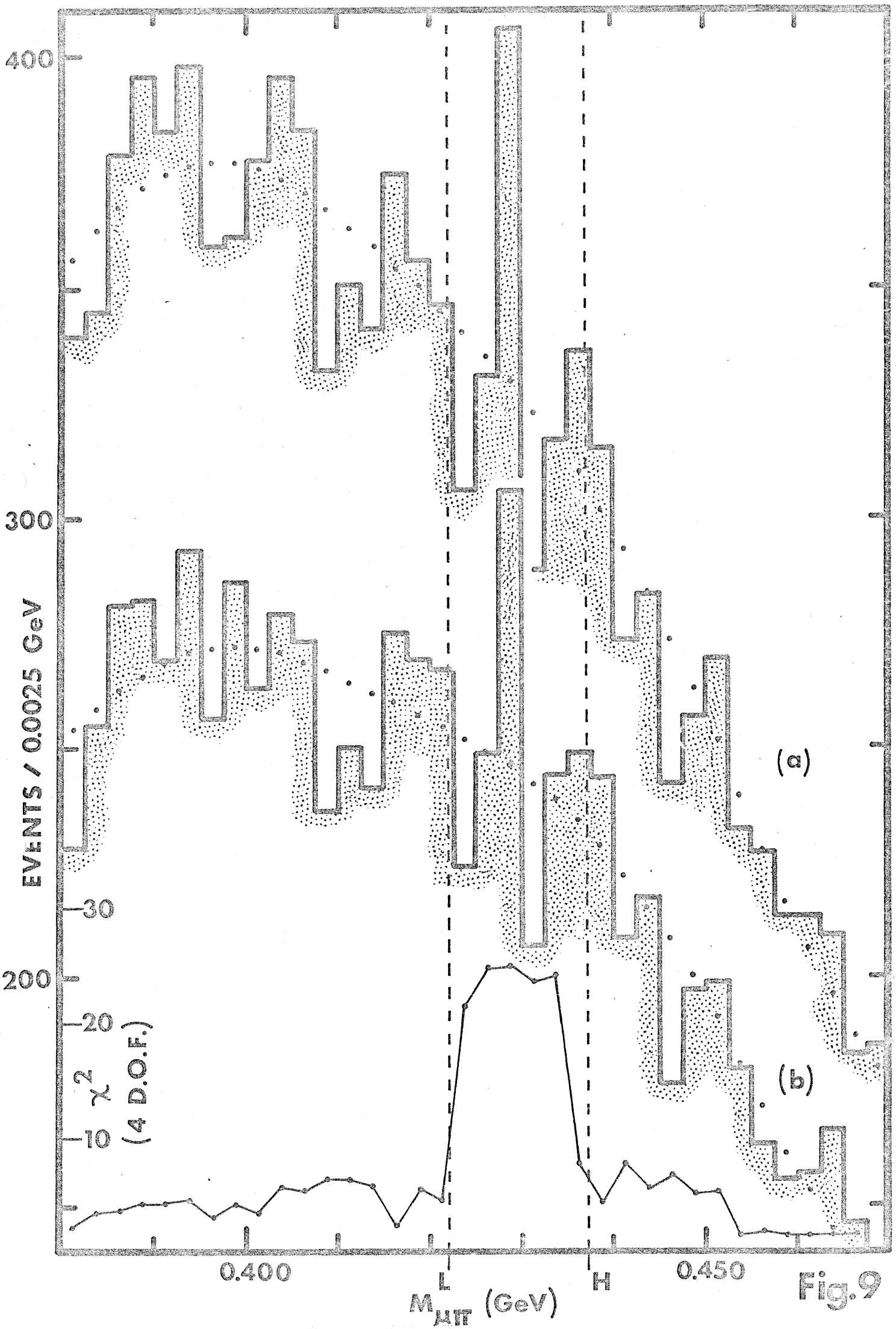
400
300
200
EVENTS / 0.0025 GeV
(a)
(b)
30
20
10
χ^2 (4 D.O.F.)
0.400
0.450
L
H
$M_{\mu\mu\pi}$ (GeV)

Fig. 9

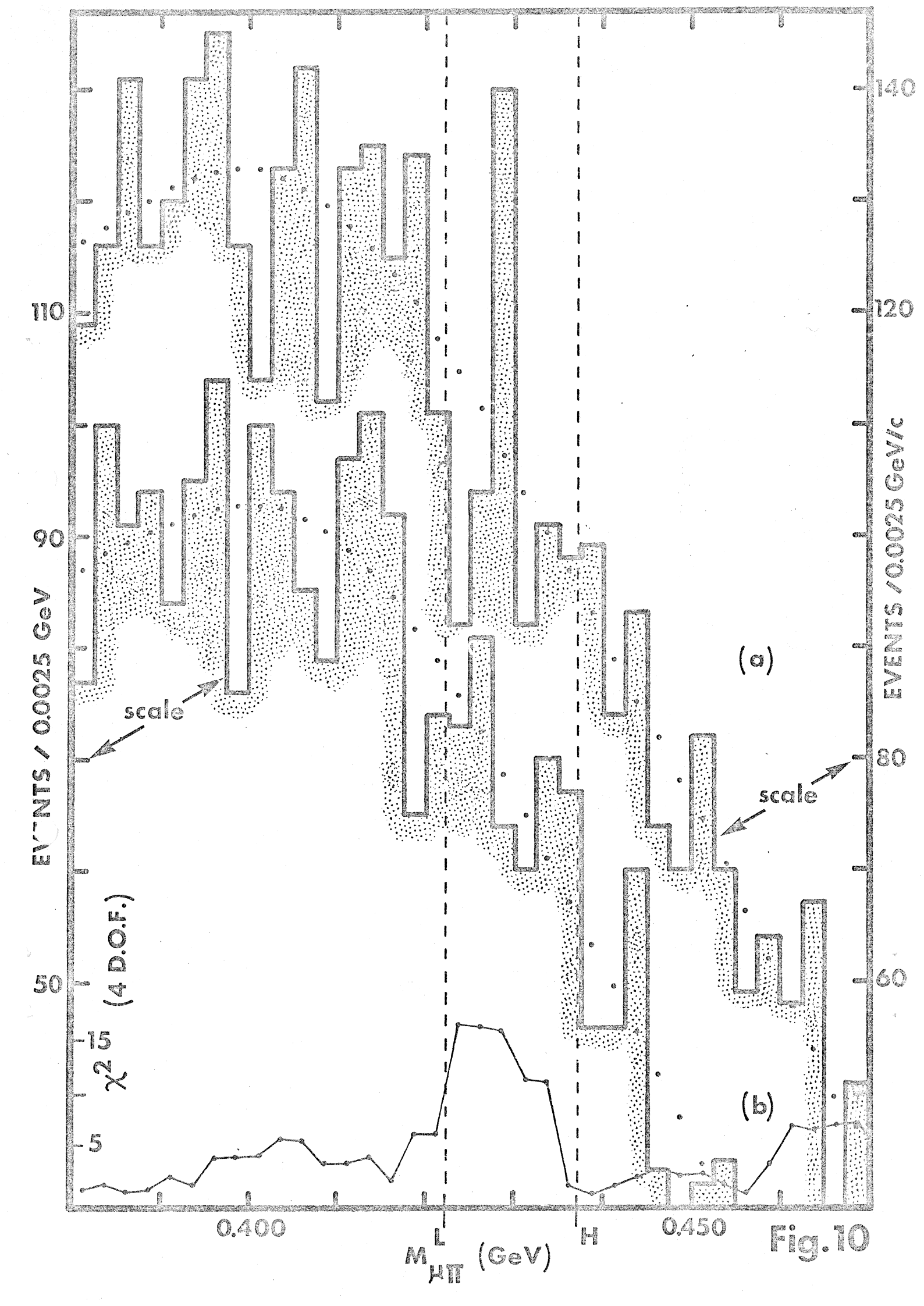
EVENTS / 0.0025 GeV
EVENTS / 0.0025 GeV/c
110
90
50
140
120
80
60
scale
scale
(a)
(b)
(4 D.O.F.)
χ^2
15
5
0.400
0.450
L
H
$M_{\mu\pi}$ (GeV)

Fig. 10